1530 *Macromolecules* **2010**, *43*, 1530–1538
DOI: 10.1021/ma902558f

Macromolecules
ARTICLE

Evidence of Strain Hardening in DNA Gels

Nermin Orakdogen,[†] Burak Erman,*[,‡] and Oguz Okay*[,†]

[†]*Department of Chemistry, Istanbul Technical University, 34469 Istanbul, Turkey and* [‡]*Department of Chemical and Biological Engineering, Koc University, 34450 Istanbul, Turkey*

Received November 20, 2009; Revised Manuscript Received December 21, 2009

ABSTRACT: Strain hardening observed in many biological gels is nature's defense against the external forces to protect the tissue integrity. Here, we show that double-stranded (ds) DNA gels also stiffen as they are strained. Chemical DNA gels were prepared by solution cross-linking of ds-DNA (about 2000 base pairs long) using the cross-linker ethylene glycol diglycidyl ether (EGDE), while physical DNA gels were prepared by the heating−cooling cycles. Stress relaxation experiments show that strain hardening in both chemical and physical gels starts to appear at 40% deformation, the extent of which increases when the amplitude of the deformation is increased up to the yield strain amplitude. The degree of strain hardening greatly depends on the contour length L_c of DNA network strands as well as on the time scale of the measurements; the gel exhibits strong strain hardening at short time scales and soften at long time scales. The maximum degree of hardening appears if the contour length of the network chains approaches 100 nm, which is the Kuhn length of ds-DNA. DNA gels exhibit universal scaled stiffening behavior that can be reproduced by a wormlike chain model taking into account the entropic elasticity of DNA strands. The results of our experiments also show that chemical DNA gels exhibit liquidlike response at strain amplitudes above 1000%, but reversibly, if the force is removed, the solution turns back to the gel state. The partial recovery of the initial microstructure of gels suggests stress-induced denaturation of ds-DNA network strands.

Introduction

Many biological gels exhibit viscoelastic properties greatly differing from those of synthetic gels of flexible polymers.[1−3] For example, mechanical response of fibrin gel, the major constituent of blood clots, is highly nonlinear, and it exhibits an increase in elastic modulus at strain amplitudes above 10%.[4] Gels formed from cytoskeletal and extracellular proteins also stiffen as they are strained, so that they resist large deformations to protect the tissue integrity.[5] Biological gels exhibiting strain hardening behavior consist of semiflexible filaments with persistence length l_p close to their contour length L_c. Thus, the filaments are only slightly coiled between the junction zones so that, even at a modest strain, their end-to-end distance r approaches their contour length L_c. According to the wormlike chain model, the force f required to separate the end-to-end distance of a semiflexible polymer by r is given by[6]

$$f = \frac{3kTr}{2L_c l_p} \tag{1a}$$

where kT is the thermal energy. Below the characteristic force kT/l_p, since the extension r is small compared to L_c, the polymer exhibits a linear elastic behavior. For flexible polymers with Kuhn length below 1 nm, this characteristic force is relatively large (a few piconewtons) so that the linear viscoelastic regime generally extends more than 100% deformations. In contrast, however, the characteristic force for semiflexible filaments such as fibrin and F-actin with persistence lengths of a few micrometers is much smaller so that nonlinear elasticity is observable even at very small deformations. For the nonlinear regime, an approximate interpolation formula for the wormlike chain force versus extension is given by[6]

$$f = \frac{kT}{l_p}\left[\frac{1}{4(1-r/L_c)^2} - \frac{1}{4} + \frac{r}{L_c}\right] \tag{1b}$$

showing that the force needed to extend a semiflexible polymer diverges as $f \sim (1-r/L_c)^{-2}$ as $r \to L_c$. The degree of strain stiffening as well as the strain, at which stiffening becomes significant, depend on the persistence length of the filament. Stiffer filaments such as F-actin or collagen stiffen at a few percent strains while more flexible filaments such as vimentin stiffen only at larger strains, approaching 100%.[5]

Deoxyribonucleic acid (DNA) in its native form is a semiflexible polymer with a double-helical conformation stabilized by hydrogen bonds between the amine bases.[7] The persistence length l_p of DNA is 50 nm,[8−10] which is much smaller that the strain stiffening proteins.[2,4,5] At concentrations below the critical overlap concentration, DNA form viscous structures in aqueous solutions, while at high concentrations, DNA molecules overlap and entangle to form a weak viscoelastic gel.[11] Only a few reports exist in the literature on the viscoelastic properties of DNA solutions. The linear viscoelastic moduli of DNA solutions have been measured by Mason et al. in the concentration range 0.1−1.0% w/v.[11] It was shown that the solutions in saline buffer behave as an entanglement network of semiflexible coils exhibiting an elastic modulus and a crossover frequency that vary with concentration according to known scaling laws.[11,12] When a DNA solution is subjected to high temperature, the hydrogen bonds holding the two strands together break and the double helix dissociates into two single flexible strands having a random coil conformation. Sun et al. showed that heating of semidilute solutions of DNA (0.5% w/v) leads to a decrease of the elastic

*To whom correspondence should be addressed.

 Published on Web 01/07/2010

modulus, indicating that the rigid-rod-like DNA molecules lost their rigidity due to the dissociation of the two strands.[12,13] Thus, the semiflexible ds-DNA consisting of fragments of about 150 base pairs behaving as rigid segments becomes flexible on heating so that the viscosity of the solution decreases.

Although nonlinear elasticity, and specifically strain stiffening, seem to be general to any network composed of semiflexible filamentous proteins, the strain hardening phenomenon in DNA has not been observed before. Since strain hardening could be facilitated by reducing the contour length L_c of the chain, one may imagine that cross-linking of DNA strands in a homogeneous solution, that is, reducing the distance between cross-link points, should produce DNA gels with stiffing properties. Soft materials such as those exemplified by DNA gels are good candidates for use in applications such as coil−globule transition, biocompatibility, selective binding, and molecular recognition.[14,15] Increasing the resistance of DNA gels against external forces will further support their potential applications, including drug and gene delivery, selective sorbents, and biosensors.

To shed some light on the nonlinear rheology of DNA, we have undertaken a systematic study of DNA gels, in which the contour length L_c of DNA network strands is varied over a wide range. Several DNA gels with a modulus of elasticity between 10^1 and 10^4 Pa were prepared by use of two techniques we recently described:[16,17]

(1) Chemical cross-linking of DNA: Solution cross-linking of DNA at 50 °C using the cross-linker ethylene glycol diglycidyl ether (EGDE) in the presence of TEMED catalyst leads to the formation of DNA gels with tunable viscoelastic properties.[16] EGDE contains epoxide groups on both ends that can react with the amino groups on the nucleotide bases to form a three-dimensional DNA network. A high concentration of DNA in the gelation solution, such as 9.3% w/v used in this study, stabilizes double-stranded (ds) DNA conformation so that ds-DNA gels were obtained.[17]

(2) Physical cross-linking of DNA by the heating−cooling cycle: Heating of semidilute solutions of ds-DNA above its melting temperature results in the dissociation of the double helix into flexible single-strand fragments.[16] On cooling back to the room temperature at a slow rate, the dissociated strands cannot reorganize to form the initial double-stranded conformation. Hence, the hydrogen bonds formed between strands belonging to different ds-DNA molecules act as physical junction zones leading to the formation of gels with a modulus of elasticity between 10^1 and 10^4 Pa.[17]

In the present study, DNA gels prepared by both techniques were subjected to various stresses, and their responses were monitored at various time scales. In the nonlinear elastic regime, since large-amplitude oscillatory measurements are inaccurate as the response waveforms are not sinusoidal,[1] we employed stress-relaxation measurements; i.e., a constant deformation was applied to the gel samples, and the resulting relaxation modulus was measured as a function of time. This technique provided insight into the dynamics of DNA network strands under shear. The degree of strain hardening depending on the contour length of DNA strands as well as on the experimental time scale was investigated. As will be seen below, DNA gels formed under certain conditions exhibit strong strain-hardening behavior, which can be quantitatively reproduced by a simple parameter-free wormlike chain model taking into account the entropic elasticity of ds-DNA strands. Further, a reversible gel−sol transition was observed in chemical DNA gels subjected to high strains, suggesting stress-induced dissociation of the double-helical network chains into flexible single strands having a random coil conformation.

Experimental Part

Materials. DNA hydrogels were made from DNA sodium salt from salmon testes (Sigma). According to the manufacturer, the % G-C content of the ds-DNA used is 41.2%, and the melting temperature is reported to be 87.5 °C in 0.15 M sodium chloride plus 0.015 M sodium citrate. The molecular weight determined by ultracentrifugation is 1.3×10^6 g/mol, which corresponds to ~2000 base pairs. The cross-linker EGDE (Fluka), the catalyst TEMED (Merck), and sodium bromide (NaBr, Merck) were used as received.

Cross-Linking Reactions. Chemically and physically cross-linked DNA gels were prepared between the parallel plates of the rheometer (Gemini 150 rheometer system, Bohlin Instruments) equipped with a Peltier device for temperature control. The upper plate (diameter 40 mm) was set at a distance of 500 μm before the onset of the reactions. Chemical DNA gels were also prepared within the rheometer equipped with a cone-and-plate geometry with a cone angle of 4° and diameter of 40 mm. During all rheological measurements, a solvent trap was used to minimize evaporation. Further, the outside of the upper plate was covered with a thin layer of low-viscosity silicone oil to prevent evaporation of solvent.

For the physical cross-linking reactions, DNA was first dissolved in 4.0 mM NaBr at 35 °C for 2 days and then transferred between the parallel plates of the rheometer. DNA concentration C_0 was varied between 0.5 and 17% w/v. The solution between the plates of the rheometer was heated from 25 to 90 °C with a heating rate of 3.25 °C/min, kept at 90 °C for 10 min, subsequently cooled down to 25 °C with a rate of 1.08 °C/min, and finally kept at 25 °C for 40 min. Each heating−cooling cycle was carried out twice to check the reproducibility of the results. Figure 1A shows typical gelation profiles of DNA solutions at three different DNA concentrations. Here, the elastic modulus G' (symbols) and the temperature of the DNA solution (red curves) are plotted against the heating−cooling time. The vertical dashed lines represent the transitions between isothermal to nonisothermal periods. During the heating period and particularly above 70 °C, G' rapidly decreases due to the dissociation of ds-DNA strands,[16] while on cooling back to 25 °C, G' dramatically increases due to the formation of cross-linking zones in the solution. Using this technique, gels with various viscoelastic properties were prepared by varying the DNA concentration C_0. Parts B and C of Figure 1 show the elastic modulus G' and the loss factor $\tan\delta$ ($= G''/G'$) of DNA solutions, respectively, before (open symbols) and after the heating−cooling cycle (filled symbols) as functions of C_0. Increasing C_0 from 0.5 to 10% also increases both G' and its fractional increase after the heating−cooling cycle so that gels with an elastic modulus between 10^1 and 10^4 Pa were obtained. This increase in the modulus with concentration is due to the increasing probability of hydrogen bond formation between portions of DNA strands belonging to different ds-DNA molecules, leading to the formation of increasing number of elastically effective DNA network chains.[18] The quantity $\tan\delta$ represents the ratio of dissipated energy to stored energy during one deformation cycle. Figure 1C also shows that, at or below 10% DNA, $\tan\delta$ is lower than that measured before the cycle, and it approaches a minimum value of about 10^{-2} at 3% DNA, indicating increasing elastic response of DNA strands after the cycle. At higher DNA concentrations, G' starts to decrease while $\tan\delta$ increases after the cycle due to the incomplete melting of DNA during the heating step.[16]

For the chemical cross-linking reactions, DNA dissolved in 4.0 mM NaBr, as described above, was mixed with TEMED catalyst (0.44% v/v) and then with various amounts of EGDE. The DNA concentration (C_0) at cross-linking was 9.3% w/v. The cross-linker (EGDE) content of the reaction solution was expressed as EGDE %, which represents the mass of pure EGDE per 100 g of DNA. The solution was then transferred between the temperature-controlled parallel plates of the rheometer. The cross-linking reactions were carried out in the rheometer at 50 °C for 3 h. Figure 1D shows typical gelation profiles of the reaction systems with 10 and 25% EGDE, where

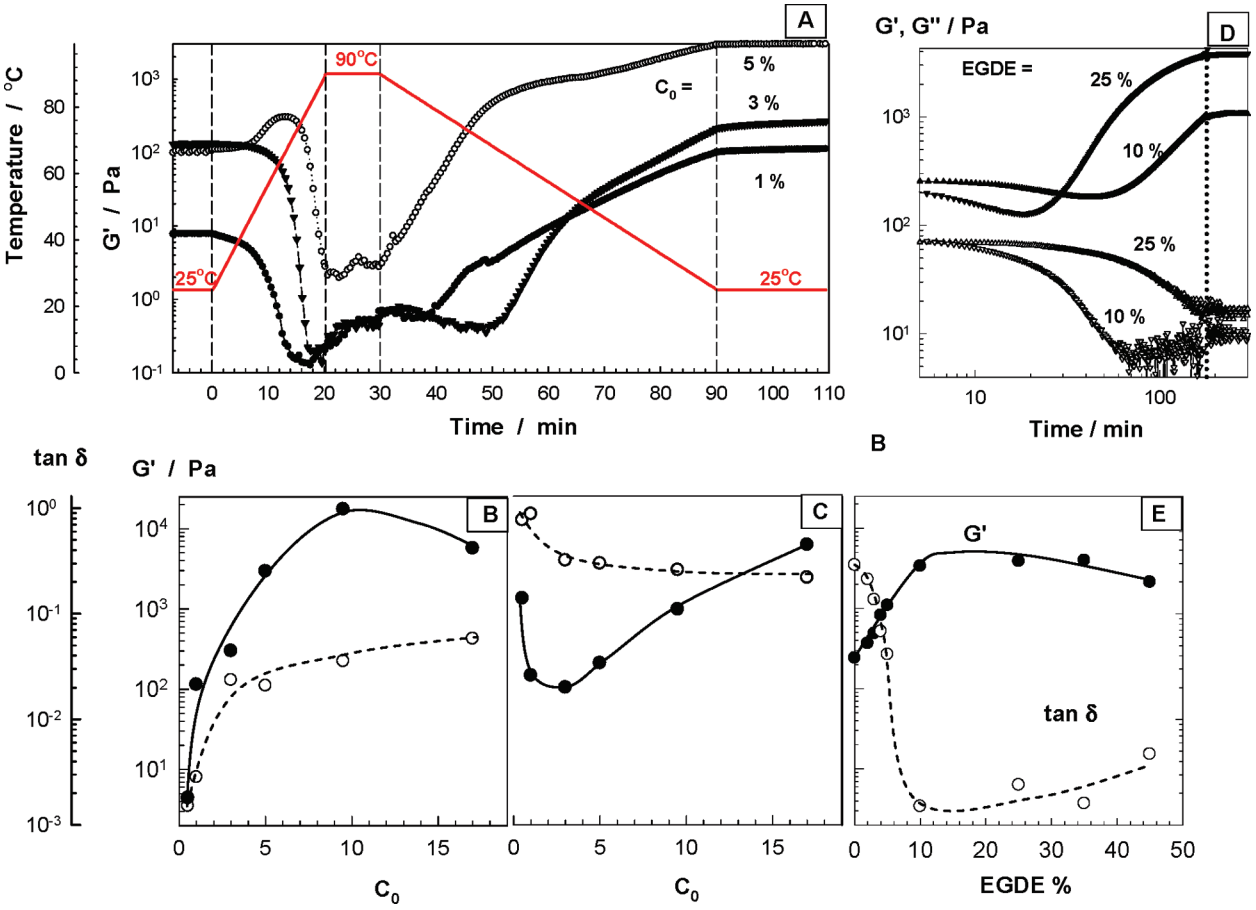

Figure 1. (A) Elastic modulus G' (symbols) and the temperature of DNA solution (red curves) shown as a function of the heating−cooling time. DNA concentrations C_0 (in % w/v) are indicated. (B, C) G' (B) and the loss factor tan δ (C) of DNA solutions before (open symbols) and after the heating−cooling cycle (filled symbols) shown as a function of C_0. (D) G' (filled symbols) and the viscous modulus G'' (open symbols) during the chemical cross-linking of ds-DNA at C_0 = 9.3%. TEMED = 0.44%. EGDE contents indicated. The dotted vertical line represents the transition from the isothermal reaction period at 50 °C to that at 25 °C. (E): G' (filled symbols) and tan δ (open symbols) of DNA gels shown as a function of EGDE concentration. C_0 = 9.3%. TEMED = 0.44%. All measurements were conducted at ω = 6.28 rad/s and γ_0 = 0.01.

the elastic moduli G' (filled symbols) and the viscous moduli G'' (open symbols) are plotted against the reaction time. A frequency of ω = 6.28 rad/s and a deformation amplitude γ_0 = 0.01 were selected for the measurements to ensure that the oscillatory deformation is within the linear regime. As reported before,[16] gelation is characterized by an initial lag phase, during which both moduli remain almost unchanged, followed by a log phase during which G' rapidly increases while G'' decreases. After 3 h of the reaction time, shown in the figure by the dotted vertical line, the temperature was reduced to 25 °C. Both moduli keep almost unchanged during this second isothermal period, indicating that the cross-linking reactions stop by reducing the temperature. Using this procedure, several gels were prepared by varying the cross-linker concentration between 2 and 45%. As seen in Figure 1E, where G' and tan δ of gels are plotted against EGDE %, gels with an elastic modulus ranging from 10^2 to 10^3 Pa and tan δ = 10^{-1}−10^{-3} were obtained.

After formation of chemical and physical gels of DNA, frequency- and strain-sweep tests (in both up and down directions) were carried out at γ_0 = 0.01 and ω = 6.28 rad/s, respectively.

Stress-Relaxation Experiments. DNA gels formed between the parallel plates were subjected to stress-relaxation experiments at 25 °C. An abrupt shear deformation of controlled strain amplitude γ_0 was applied to the gel samples, and the resulting stress $\sigma(t,\gamma_0)$

$$\sigma(t,\gamma_0) = \gamma_0 G(t,\gamma_0) \qquad (2)$$

was monitored as a function of time. The time t after application of step deformation represents a time scale that describes the motion of the DNA strands in the network and is equivalent to the inverse of the frequency ω in an oscillatory test. Here, we report the relaxation modulus $G(t,\gamma_0)$ as functions of the relaxation time t and strain amplitude γ_0. The experiments were conducted with increasing strain amplitudes γ_0 from 0.01 to 10. For each DNA gel, stress-relaxation experiments at various γ_0 were conducted starting from a value of the relaxation modulus deviating less than 10% from the modulus measured at γ_0 = 0.01. Measurements with chemical DNA gels were also carried out with the rheometer equipped with a cone-and-plate geometry with a cone angle of 4° and diameter of 40 mm. The data obtained using both geometries were reproducible with a relative error of less than 15%.

Results and Discussion

Chemical and physical gels of DNA were prepared by use of two techniques described in the Experimental Part. For the physical cross-linking of DNA, the main experimental parameter was the DNA concentration C_0, which was varied between 0.5 and 17%. For the chemical cross-linking of DNA, C_0 was set to 9.3% to prevent denaturation while the cross-linker (EGDE) concentration was varied between 2 and 45%. After a steady state was reached, that is, after both the elastic G' and the viscous moduli G'' reached steady-state plateau independent of time, frequency-sweep tests at a strain amplitude γ_0 = 0.01 were carried out (Figure S1). Both techniques lead to the formation of weak to strong DNA gels depending on the experimental parameters. As reported before,[16,17] no substantial denaturation of DNA occurs under the reaction conditions so that the gels formed

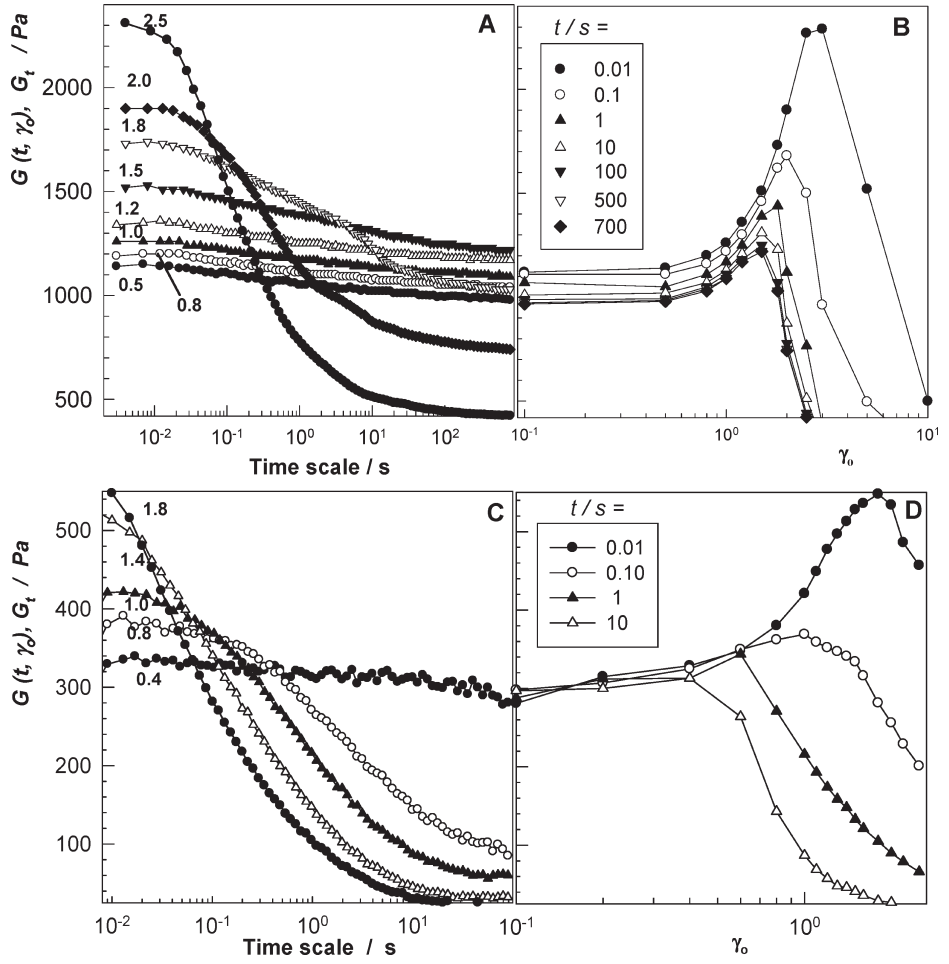

Figure 2. Relaxation modulus $G(t,\gamma_0)$ of chemical (A) and physical DNA gels (C) as a function of time scale for various strain amplitudes γ_0 indicated. Chemical DNA gel was prepared at 5% EGDE while the physical gel was prepared at C_0 = 3%. Parts B and D were derived from parts A and C, respectively, and show the relaxation modulus G_t at given time scale t as a function of γ_0.

consist of ds-DNA network strands. The gels were then subjected to stress-relaxation experiments. We discuss the results of our observations in three subsections. In the first subsection, strain hardening behavior of DNA gels is demonstrated, while in the second subsection the results are explained using a wormlike chain model taking into account the entropic elasticity of DNA network chains. In the last subsection, the possibility of stress-induced denaturation of DNA strands in gels is demonstrated by strain-sweep tests, and the experimental observations are interpreted.

Strain Hardening. Strain-dependent properties of DNA gels were measured by stress-relaxation experiments. The stress $\sigma(t,\gamma_0)$ was monitored after application of a shear deformation of controlled amplitude γ_0 for a duration of 700 s. Parts A and C of Figure 2 show typical relaxation profiles of chemical (5% EGDE) and physical DNA gels (C_0 = 3%), respectively, where the relaxation modulus $G(t,\gamma_0)$ is shown as a function of time scale t for various strain amplitudes γ_0. The most noticeable result is the increase of the modulus with deformation at time scales below 10^{-1} s (strain hardening), while at longer time scales, it decreases with deformation (strain softening). Further, at low strain amplitudes, i.e., between γ_o = 0.5 and 1.5 for the chemical gel, the time dependence of $G(t,\gamma_0)$ appears to be rather similar. When the deformation exceeds a critical value of γ_0, which is 1.5 and 0.4 in parts A and C of Figure 2, respectively, the overall relaxation becomes faster. The DNA strands in this regime first relax rapidly but then slowly reach a quasi-plateau at longer times.

In Figure 2B,D, the relaxation moduli G_t at a given time scale t are plotted as a function of the strain amplitude γ_0. DNA gels are in the linear regime; that is, the modulus G_t is independent of strain for γ_0 below 40%, while they exhibit strain hardening for γ_0 between 40 and 250%, before softening at higher strains. The shorter the time scale, the larger the degree of strain hardening and the larger the yield strain γ_c, i.e., the strain at which the modulus starts decreasing. At time scales t shorter than 0.10 s, that is, at high rates of shear ω > 1 rad/s, strain hardening was pronounced and G_t increased up to 100% compared to its value at low strains. Another interesting point shown in Figure 2 is the large decrease of the modulus at high strains even in chemically cross-linked DNA gels, which will be discussed later.

Similar plots such as those given in Figure 2 were also obtained for other physical and chemical DNA gels formed under various experimental conditions (Figure S2). Among the physical gels, the maximum degree of strain hardening and the largest yield strain γ_c were observed for those formed at C_0 = 3%, i.e., for gels exhibiting a minimum value of loss factor (Figure 1C). At high DNA concentrations, at which the elastic modulus exceeds 10 kPa, the gels exhibited strain softening behavior. For example, Figure 3A shows strain-dependent moduli G_t versus strain amplitude γ_0 plots for the physical gel formed at C_0 = 17% before and after the heating−cooling cycle. Although the modulus of the DNA gel increases about 1 order of magnitude due to the heating−cooling cycle, the additional cross-links formed

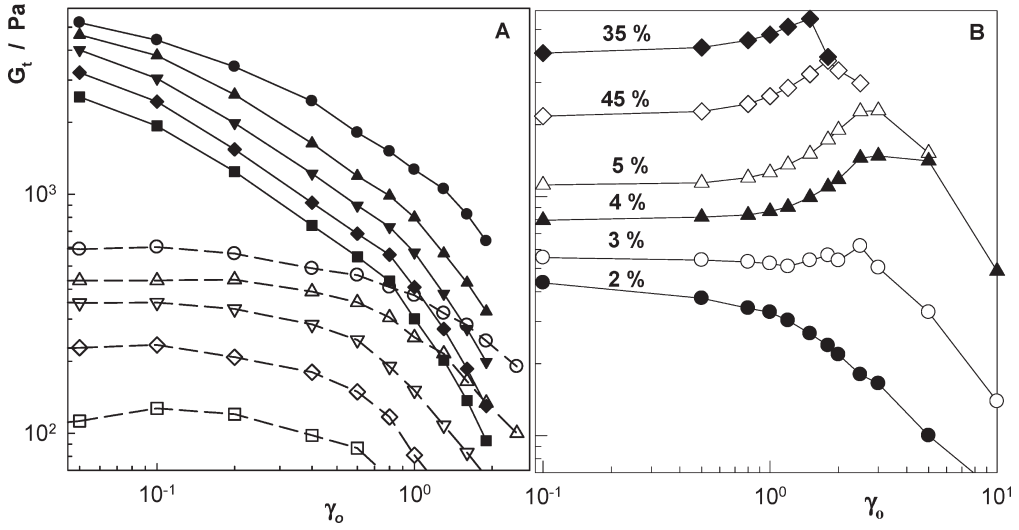

Figure 3. Strain-dependent modulus G_t of DNA gels as a function of strain amplitude γ_0 . (A) Physical gels before (open symbols) and after the heating−cooling cycle (filled symbols). C_0 = 17%. Time scale = 0.01 (●, ○), 0.1 (▲, △), 1 (▼, ▽), 10 (◆, ◇), and 90 s (■, □). (B) Chemical gels at various EGDE contents indicated. Time scale = 0.01 s.

seem to be too weak so that they easily dissociate even at strains below 10%. Figure 3B shows the moduli G_t of chemical gels after a time scale of 0.01 s plotted against the strain amplitude γ_0 for various cross-linker contents. Loosely cross-linked gels soften on deformation while strain hardening appears at higher cross-linker contents, the extent of which as well as the yield strain increases up to a critical cross-linker content (5%) but then decreases again.

Let $G_{t,\max}$ be the maximum value of the relaxation modulus achieved during deformation; hardening % can be calculated as $(G_{t,\max}/G_0 - 1) \times 10^2$, where G_0 is the modulus in the linear regime. In Figure 4A,B, hardening % observed at a time scale of 0.01 s is plotted against G_0 and tan δ of chemical (filled symbols) and physical DNA gels (open symbols). Since most of the physical gels of DNA exhibit strain softening (Figure S2), a clear correlation between the hardening behavior and the gel elasticity is only seen in chemical DNA gels; a maximum degree of hardening (> 100%) was observed in gels exhibiting an elastic modulus of about 1 kPa and a loss factor of 0.05. Assuming that G_0 corresponds to the equilibrium shear modulus G, one may estimate the molecular weight $\bar{M}_c$ of the network chains in DNA gels. G at the state of gel preparation is given for an affine network by[19,20]

$$G = (\rho/\bar{M}_c)RT\nu_2^0 \tag{3}$$

where ρ is the DNA density, ν_2^0 is the volume fraction of cross-linked DNA in the gel, and R and T have their usual meanings. Since $\rho\nu_2^0$ corresponds to the DNA concentration C_0 in the gel, calculations using eq 3 show that $\bar{M}_c$ decreases from 620 to 58 kg/mol as the modulus is increased from 0.37 to 4.0 kPa. Further, using the known distance between the base pairs along the chain (0.34 nm), the result implies a decrease of the contour length, i.e., of the distance between cross-links L_c from 326 to 30 nm with increasing modulus. In Figure 4C, strain hardening % is plotted against L_c. The degree of strain hardening increases as L_c is decreased starting from 300 nm. A maximum degree of hardening is observable as L_c approaches 100 nm, which is the Kuhn length, or twice the persistence length of ds-DNA. Since there is only one Kuhn chain for L_c = 100 nm, such a ds-DNA strand should behave, by definition, as a rigid rod and should exhibit infinite modulus. However, because of the spatial inhomogeneities existing in real gels,[21−23] the infinite modulus of the theory seems to appear as a maximum degree of strain hardening in our experiments. It is also interesting to see the experimental data in Figure 4C below L_c = 100 nm. Since a decrease of L_c below the Kuhn length of ds-DNA is not possible, the data suggest local opening of double-helical fragments along a Kuhn length due to the action of additional cross-links. This is schematically illustrated in the inset to Figure 4C. Since the Kuhn length of ss-DNA is about 1 nm, such openings may allow decrease of L_c below 100 nm at high cross-link densities.

A strong enhancement in the degree of strain hardening at short time scales suggests that not only the chemical cross-links but also the entanglements, where DNA network strands cross and loop around each other, play a role in the stiffening of DNA network. Permanent cross-links created chemically or physically determine the contour length L_c of the network strands. Although strain hardening appears if L_c decreases below 300 nm (Figure 4C), its extension at long time scales is low (< 50%), even at L_c values shorter than the Kuhn length of ds-DNA. Thus, not only the contour length of DNA strands but also its rigidity should be controlled to obtain strong stiffening behavior. Since the concentration of DNA in gels is well above its critical overlap concentration c^* (0.043%),[16] the strands between the cross-link points form entanglements with surrounding strands. Despite the transient nature of these entanglements, at time scales shorter than the relaxation time of strands, their effect is much the same as that of chemical cross-links, inhibiting the motion of each network chain laterally and confines it in a tubelike region.[24] For longer time scales, however, entanglements allow DNA network chains to slide past one another. Thus, both steric interactions and DNA's intrinsic rigidity are responsible for the strain-hardening behavior of DNA gels. In the following paragraphs, we show that the strain hardening of DNA gels can be explained in terms of entropic elasticity of the DNA strands.

Entropic Elasticity of DNA Strands. The elastic energy function W of a single semiflexible polymer associated with eq 1b is[25]

$$W = \frac{kTL_c}{4l_p}\left[2z^2 + \frac{1}{1-z} - z\right] + C_0 \tag{4}$$

where z is the extension ratio with respect to the contour length L_c, i.e., $z = r/L_c$, and C_0 is a constant. We redefine the

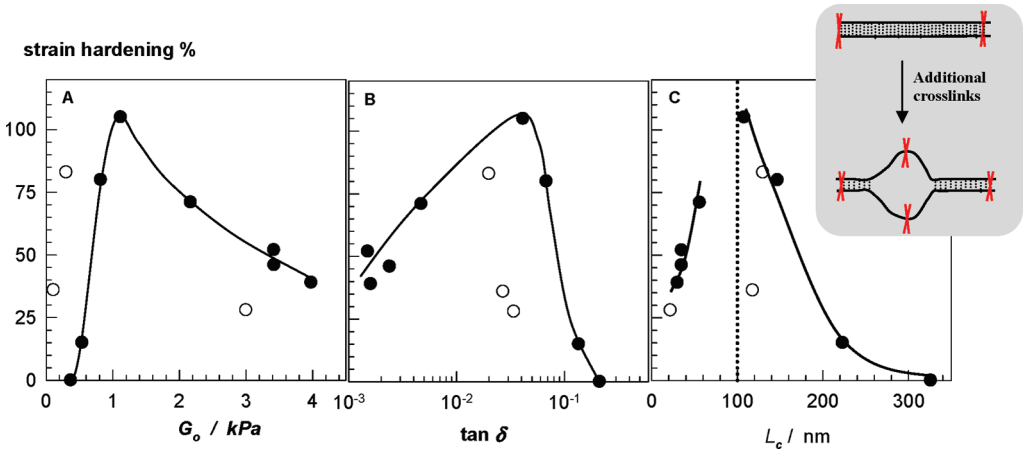

Figure 4. Degree of strain hardening at $t = 0.01$ s shown as functions of initial elastic modulus G_0 (A), the loss factor tan δ (B), and the length L_c of DNA network strands (C) for chemical (filled symbols) and physical DNA gels (open symbols). Curves are guide to the eye for the chemical gels. The dotted vertical line in (C) denotes the Kuhn length l, or twice the persistence length of ds-DNA. The inset shows opening of ds-DNA fragments between chemical cross-links represented by red crosses.

extension ratio of a chain as $\lambda_{chain} = r/r_0$, where r_0 is the end-to-end distance of a freely jointed chain consisting of N Kuhn segments each of length l, i.e., $r_0 = N^{1/2}l$. Since $L_c = Nl$, the extension ratio z is related to λ_{chain} by

$$z = \lambda_{chain}/\sqrt{N} \tag{4a}$$

Let us now consider a coordinate system in which one end of the chain is affixed at the origin and the other end is such that the end-to-end vector makes direction cosines $m_x = \cos\theta_x$, $m_y = \cos\theta_y$, $m_z = \cos\theta_z$ with the coordinate axes. Then, the extension ratio of the chain will be ${\lambda_{chain}}^2 = \sum_{k=1}^{3} m_k{}^2 {\lambda_k}^2$, where λ_k is the extension ratio along the kth coordinate direction. Assuming that the chains are isotropically oriented in the undeformed network, we obtain

$${\lambda_{chain}}^2 = \frac{1}{3}\sum_{k=1}^{3} {\lambda_k}^2 = \frac{1}{3}I_1 \tag{4b}$$

Substitution eqs 4a and 4b into eq 4 leads to the energy function of a network chain subjected to a state of deformation given by I_1. In order to find the free energy of a network that is composed of ν chains, we simply add the free energies of each chain.[26,27] Further, we determine the constant C_0 in eq 4 in such a way that $W = 0$ when $I_1 = 3$. This leads to the following energy expression:

$$W = \frac{1}{2}\nu kT\left[\frac{2}{3}(I_1 - 3) + N\left(\frac{1}{1-\sqrt{\frac{I_1}{3N}}} - \frac{1}{1-\sqrt{\frac{1}{N}}} - \sqrt{\frac{I_1}{3N}} + \sqrt{\frac{1}{N}}\right)\right] \tag{5}$$

Note that since the Kuhn length l is twice the persistence length l_p, we replaced L_c in the front factor of eq 4 by $2Nl_p$. The energy diverges in two limits, when $N \to 1$ and $I_1 \to 3N$. The divergence at $N \to 1$ is expected since in this limit there is only one Kuhn chain which is equivalent to a rigid rod, and a rigid rod has infinite modulus by definition. The other limit, $I_1 \to 3N$, corresponds to $z \to 1$, i.e., full extension of the chain at which the end-to-end distance equals to the contour length. On the other hand, in the limit $N \to \infty$, the second term in eq 5 goes to $^1/_3(I_1 - 3)$, and we get $W(N\to\infty) = {}^1/_2\nu kT(I_1 - 3)$, which is the classical affine network free energy of Gaussian chains.

For simple shear, since $I_1 - 3 = {\gamma_0}^2$, the shear stress σ is obtained from eq 5 as $\sigma = G\gamma_0$, where G is the modulus. The modulus G and the reduced modulus G_r normalized with respect to the modulus at zero strain are

$$G = \frac{1}{2}(\nu/V)kT\frac{2 - 3\sqrt{\frac{I_1}{3N}} + \frac{4I_1}{9N}}{\left(1-\sqrt{\frac{I_1}{3N}}\right)^2} \tag{6}$$

$$G_r = \left[\frac{\left(1-\frac{1}{\sqrt{N}}\right)^2}{2 - \frac{3}{\sqrt{N}} + \frac{4}{3N}}\right]\left[\frac{2 - 3\sqrt{\frac{I_1}{3N}} + \frac{4I_1}{9N}}{\left(1-\sqrt{\frac{I_1}{3N}}\right)^2}\right] \tag{7}$$

where V is the volume of the network. In Figure 5A, the reduced modulus G_r predicted by eq 7 is plotted against strain γ_0, i.e., against $(I_1 - 3)^{1/2}$, for various N between 1.01 and 100. G_r goes to infinity as $\gamma_0 \to [3(N-1)]^{1/2}$ corresponding to the limit $z \to 1$, i.e., to the full extension of the chain. As a consequence, strain hardening appears at a lower strain as N is decreased, that is, as the contour length L_c of the chain decreases.

To obtain a universal relation between the reduced modulus G_r and the strain γ_0, we define a new measure of strain

$$y = \sqrt{\frac{I_1}{N}} \tag{8}$$

Equation 7 can then be written as

$$G_r(N, y) = C(N)g(y) \tag{9}$$

where $C(N)$ and $g(y)$ are the first and the second terms on the right-hand side of eq 7. Let us now scale the argument of $g(y)$ by y_0. In the scaling limit, we can write eq 9 as

$$G_r(N, y) = C(N){y_0}^m g\left(\frac{y}{y_0}\right) \tag{10}$$

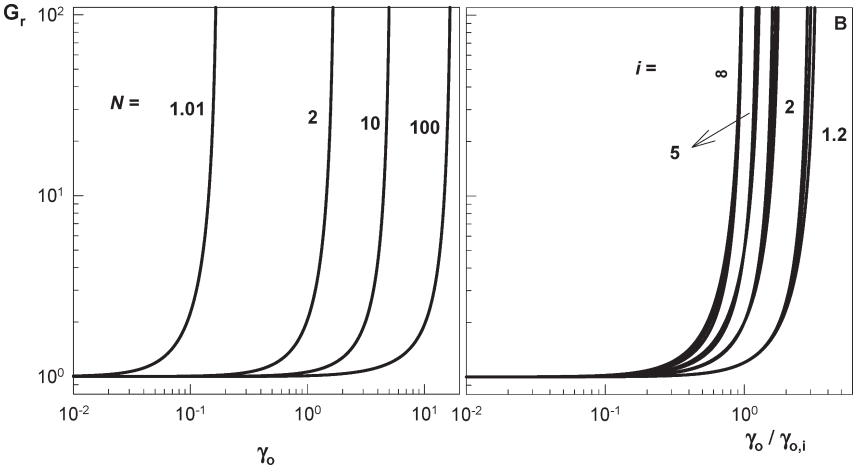

Figure 5. (A) Reduced modulus G_r predicted by eq 7 shown as a function of strain γ_0 for various N between 1.01 and 100. (B) G_r plotted against strain γ_0 normalized by the strain $\gamma_{0,i}$ at which $G_r = i$. The values i are indicated. Calculations were for N between 1.01 and 100.

where m is the scaling exponent. For the condition $y = y_0$, we have $g(1) \cong 4$ from eq 7, and ${y_0}^m = G_r(N,y_0)/(4C(N))$ so that eq 10 can be written as

$$\frac{G_r(N,y)}{G_r(N,y_0)} = \frac{1}{4}g\left(\frac{y}{y_0}\right) \tag{11}$$

Substituting from eq 8, we obtain

$$\frac{G_r(I_1,N)}{G_r(I_{1,0},N)} = \frac{1}{4}g\left(\frac{I_1}{I_{10}}\right) \tag{11a}$$

Since the right-hand side of eq 11a is independent of N, the left-hand side should also be independent of N. Therefore, the only possible form of $G_r(I_1,N)$ is $G_r(I_1,N) = f(N)G_r(I_1)$, where $f(N)$is a function of N only. We therefore have

$$\frac{G_r(I_1)}{G_r(I_{10})} = \frac{1}{4}g\left(\frac{I_1}{I_{10}}\right) \tag{12}$$

In terms of the strain γ_0, eq 12 suggests that the reduced modulus only depends on the normalized strain, i.e.

$$G_r \propto \frac{\gamma_0}{\gamma_{0,i}} \tag{13}$$

where $\gamma_{0,i}$ is the strain at which $G_r = i$, where i is an arbitrarily chosen value for the degree of stiffening in the scaling limit.

In Figure 5B, G_r predicted by eq 7 is plotted against $\gamma_0/\gamma_{0,i}$. Calculations are for i = 1.2, 2, 5, and ∞, while for each i, the number of Kuhn segments N was varied between 1.01 and 100. In accord with eq 13, G_r vs $\gamma_o/\gamma_{0,i}$ plots are insensitive to the values of N, i.e., to the cross-link density of gels. In Figure 6, all the experimental reduced modulus data of DNA gels are plotted against the strain γ_0 normalized by $\gamma_{0,i}$ with i = 1.2. The value i = 1.2 was chosen since most of the DNA gels exhibited, at least, this degree of strain hardening (20%). Experimental data shown in the figure are those measured below the yield stress and for all time scales between 0.01 and 10 s. It is seen that all the data fall onto the same curve independent of the type of cross-links, the degree of cross-linking, or the duration of the relaxation time; they differ only in the end point of the curve, for example, the modulus stops rising at G_r = 1.4 and 2.04 for t = 1 and 0.01 s, respectively. Such a universal relation between G_r and $\gamma_0/\gamma_{0,i}$ was also observed for actin, collagen, and fibrin protofibril networks.[5] The curves in Figure 6 were calculated using eq 7 for N values between 1.01 and 100. Slight variations between the theoretical curves are due to the fact that the reference state i = 1.2 is not in the scaling limit. However, eq 7 in combination with eq 13 forms a parameter-free equation system describing well the strain hardening behavior of all DNA gels prepared in this study. Note that the deviation between the theory and experiment at large strains is due to the fact that the experimental data points in this range of γ_0 are between the strain hardening and strain softening regimes (Figure 2 and Figure S2), where the latter is not accounted for by the theory.

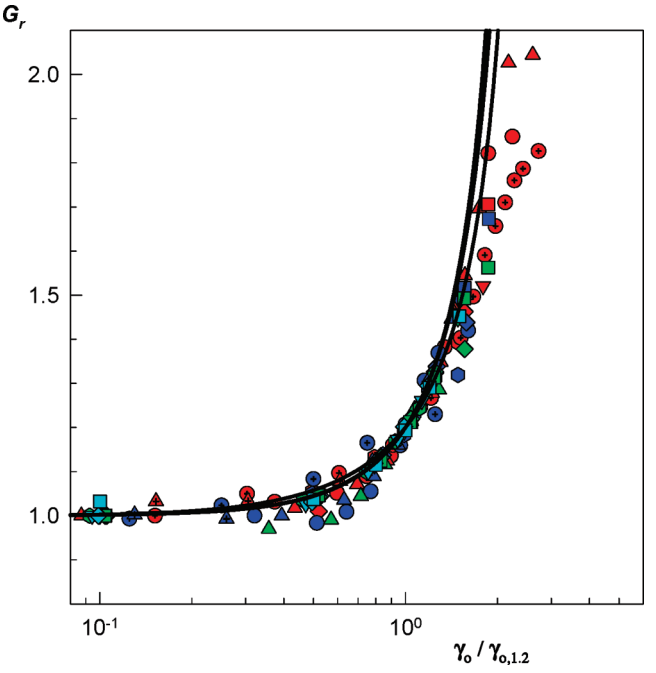

Figure 6. Reduced moduli G_r of DNA gels plotted against strain γ_0 normalized by the strain $\gamma_{0,1.2}$ at which G_r = 1.2. Chemical DNA gels: EGDE = 4 (circle), 5 (triangle up), 10 (triangle down), 25 (diamond), 35 (hexagon), and 45% (square). Physical DNA gels: C_0 = 3 (crossed circle) and 5% (crossed square). The time scales 0.01, 0.1, 1, and 10 s are shown by symbols in red, blue, green, and cyan, respectively. The curves were calculated using eq 7 for N = 1.01−100.

We have to mention that the expression for the free energy of the single chain given by eq 4 does not contain enthalpic contributions at high extensions that are

observed in experiments when semiflexible chains are overstretched.[28−31] Recently, the free energy expression for semiflexible filaments has been improved by Blondell and Terentjev to include this effect explicitly in the force−extension relation.[32] The softening due to overstretching resulting from the increase of the contour length of the chain is also observed in gels of semiflexible chains. Indeed, the deviations of experimental points from the asymptotically increasing theoretical curves at high extensions in Figure 6 result from overstretching of chains. As we have done for entropic elasticity in this paper, the single chain force−extension relation at high deformations given by Blundell and Terentjev could be incorporated into the corresponding equation for the network, in principle. However, we were not able to do this in a closed form expression. It suffices to say that the effect is clearly present in DNA gels at high extensions as evidenced in Figure 6. Further, the theoretical model presented assumes equilibrium states for DNA gels and does not describe their relaxation dynamics.[33,34]

Stress-Induced Denaturation. An interesting point shown from relaxation profiles of DNA gels is that the relaxation time rapidly decreases in the strain-hardening regime and the modulus drastically decreases at long time scales (Figure 2). A similar behavior was observed in telechelic networks made of flowerlike micelles where strain hardening and simultaneously a decrease of the viscoelastic relaxation time were observed with increasing γ_0.[35] This decrease in the relaxation time in the strain-hardening regime was ascribed to the increase of the breakage probability of nonpermanent cross-links with the stretching of the transient networks.[35] However, since the strands in chemical DNA gels are connected to each other by covalent bonds and to break a covalent bond requires much larger forces, the results cannot be explained with the rupture of interstrand cross-links of EGDE.

To explain this unusual feature of DNA gels, strain-sweep tests at a frequency $\omega = 6.28$ rad/s were conducted for strain amplitudes γ_0 ranging from 0.001 to 30. The results of the up and down strain-sweep experiments for chemical DNA gels of various linear elastic moduli are shown in Figure 7. For loosely cross-linked DNA gels with an elastic modulus of 10^2 Pa (Figure 7A), the upward and downward dynamic moduli superimpose; the gels soften with increasing deformation and exhibit liquidlike response above $\gamma_0 = 10$, but reversibly, if the force is removed, the solution turns back to the same gel state. For gels with a modulus of 10^3 Pa (Figure 7B−D), a gel-to-sol transition also occurs around $\gamma_0 = 10$, while during the downward sweep tests, the initial moduli of gels are partially recovered. Increasing the initial modulus from 1110 to 3860 Pa, i.e., increasing the cross-link density of gels, also increases the recoverability of the initial elastic modulus from 12 and 36%. Further, the viscous modulus G'' in the strain hardening regime rapidly increases with strain, suggesting that an increasing amount of energy is dissipated during this period. Such a drastic increase in G'' has been observed in networks of nanoparticles during the breakdown of agglomerates to a larger number of smaller size units, which are more dissipative.[36]

The partial recovery of the initial microstructure of DNA gels after their breakdown demonstrates that not the interstrand EGDE cross-links but the hydrogen bonds holding the two strands together break under deformation so that the double helix dissociates into two single strands having a random coil conformation. Previous experiments conducted at the single molecule level show separation of the two strands of ds-DNA by the application of a force.[37−40] The rupture of DNA molecule by unpairing of the bases occurs

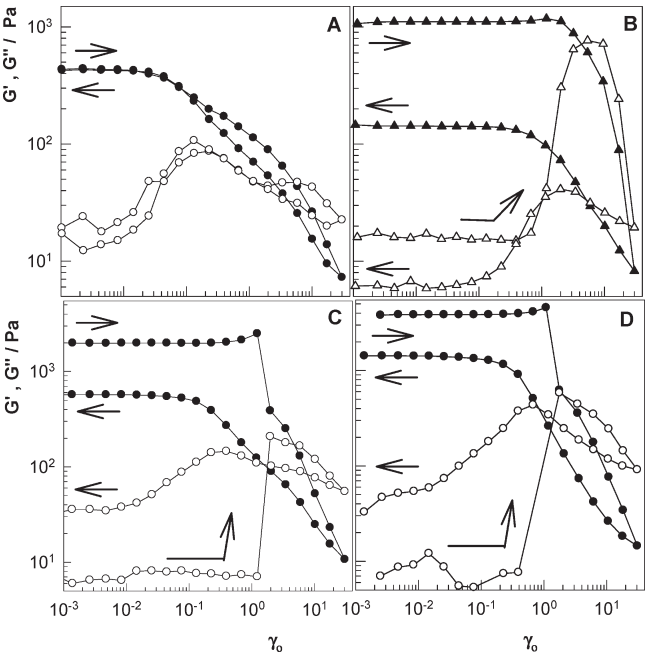

Figure 7. G' (filled symbols) and G'' (open symbols) of chemical DNA gels shown as a function of the strain γ_0 at $\omega = 6.28$ rad/s measured just after the gelation reactions. Sweep tests were conducted in up and down directions as indicated by the arrows. EGDE = 3 (A), 5 (B), 45 (C), and 25% (D).

when its extension ratio increases above 200%.[41] When the force reaches the threshold to unpair two bases (15 and 12 pN for GC- and AT-rich regions, respectively), the bond yields and the bases unbinds cooperatively. Thus, our results can be explained according to the following scenario (Figure 8): Since ss-DNA is a flexible polymer compared to semiflexible ds-DNA, dissociation of ds-DNA produces single-strand fragments of much smaller volume. Calculations show that the radius of gyration of ds-DNA of 2000 bp long is 106 nm in water, as compared to 20 nm for the corresponding ss-DNA.[16] This indicates that each DNA molecule will occupy 150-fold smaller volume after denaturation (Figure 8A). Thus, stress-induced denaturation of elastically effective semiflexible network chains will produce, depending on the location of the cross-link points on the strands, flexible network chains and free chains (sol fraction) or dangling chains (Figure 8B); in both cases, more energy is dissipated as the strain is increased and the gel becomes a liquid at high strains. On removing force, the initial microstructure is partially recovered so that the elastic modulus increases again. At high cross-link densities, since larger number of the strands are connected to each other by chemical bonds, dissociated strands can find each other easier so that the recoverability increases.

Conclusions

Stress relaxation experiments show that DNA gels stiffen as they are strained. Strain hardening in both chemical and physical DNA gels starts to appear at 40% deformation, the extent of which increases when the amplitude of the deformation is increased up to the yield strain amplitude. The degree of strain hardening greatly depends on the contour length L_c of DNA network strands as well as on the time scale of the measurements; the gel exhibits strong strain hardening at short time scales and soften at long time scales. The maximum degree of hardening appears if the contour length of the network chains approaches 100 nm, i.e., to the Kuhn length of ds-DNA. DNA gels exhibit

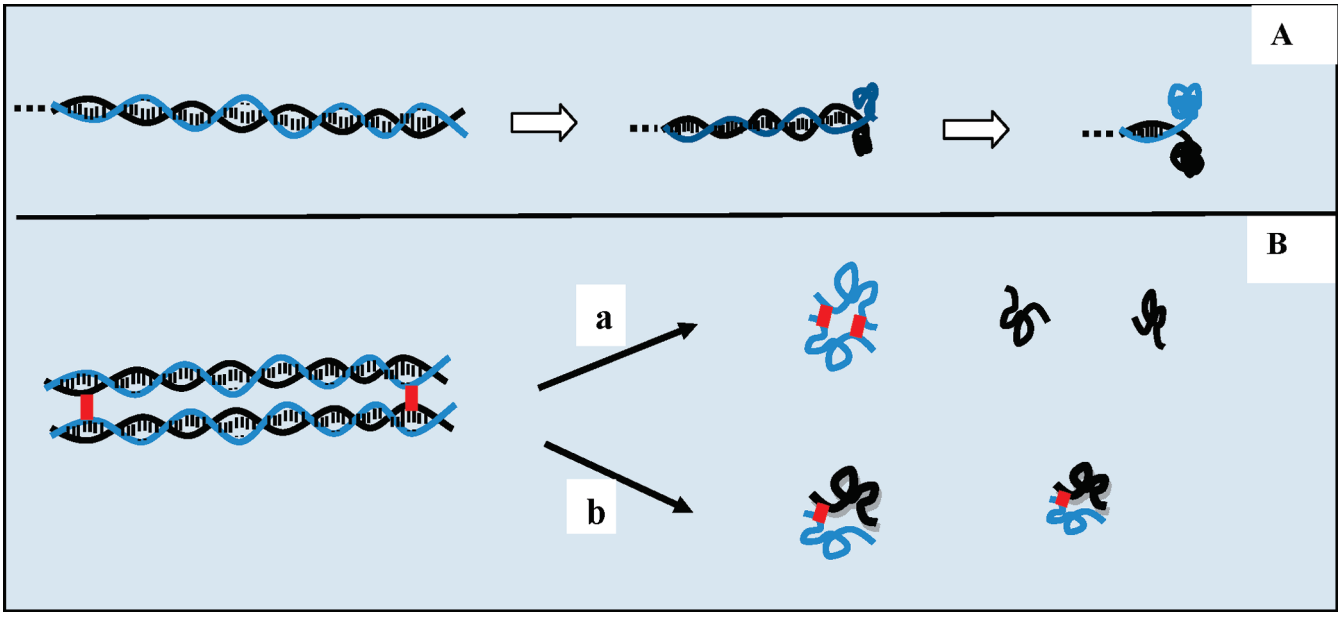

Figure 8. Cartoon demonstrating stress-induced denaturation of DNA (A) and gel−sol transition of DNA gel under deformation (B). In (B), the cross-links are shown by red lines. If the cross-link points are on the same strand of the double helix (route a), flexible network chains together with single ss-DNA strands will form. Otherwise (route b), denaturation results dangling chains in the gel.

universal scaled stiffening behavior that can be reproduced by a wormlike chain model taking into account the entropic elasticity of DNA strands. The results of our experiments also show that chemical DNA gels exhibit liquidlike response at strain amplitudes above 1000%, but reversibly, if the force is removed, the solution turns back to the gel state. The partial recovery of the initial microstructure of gels suggests stress-induced denaturation of ds-DNA network strands.

Acknowledgment. This work was supported by the Scientific and Technical Research Council of Turkey (TUBITAK). O.O. and B.E. thank Turkish Academy of Sciences (TUBA) for partial support.

Supporting Information Available: Figure S1 showing the mechanical spectra of DNA gels formed by physical and chemical cross-linking reactions and Figure S2 showing the relaxation modulus G_t of DNA gels at 25 °C shown as a function of strain γ_0. This material is available free of charge via the Internet at http://pubs.acs.org.

References and Notes

(1) Xu, J.; Tseng, Y.; Wirtz, D. J. *J. Biol. Chem.* **2000**, *275*, 35886.
(2) Gardel, M. L.; Shin, J. H.; MacKintosh, F. C.; Mahadevan, L.; Matsudaira, P.; Weitz, D. A. *Science* **2004**, *304*, 1301.
(3) Gardel, M. L.; Kasza, K. E.; Brangwynne, C. P.; Liu, J.; Weitz, D. A. *Methods Cell Biol.* **2008**, *89*, 487.
(4) Shah, J. V.; Janmey, P. A. *Rheol. Acta* **1997**, *36*, 262.
(5) Storm, C.; Pastore, J. J.; MacKintosh, F. C.; Lubensky, T. C.; Janmey, P. A. *Nature* **2005**, *435*, 191.
(6) Marko, J. F.; Siggia, E. D. *Macromolecules* **1995**, *28*, 8759.
(7) Xu, J.; LaBean, T. H.; Craig, S. L. In *Supramolecular Polymers*; Ciferri, A., Ed.; CRC Press: Boca Raton, FL, 2004; Chapter 12, p 445.
(8) Hagerman, P. J. *Annu. Rev. Biophys. Biophys. Chem.* **1988**, *17*, 265.
(9) Tothova, J.; Brutovsky, B.; Lisy, V. *Eur. Phys. J. E* **2007**, *24*, 61.
(10) Tinland, B.; Pluen, A.; Sturm, J.; Weill, G. *Macromolecules* **1997**, *30*, 5763.
(11) Mason, T. G.; Dhople, A.; Wirtz, D. *Macromolecules* **1998**, *31*, 3600.
(12) Sun, M.; Pejanovic, S.; Mijovic, J. *Macromolecules* **2005**, *38*, 9854.
(13) Rice, S. A.; Doty, P. *J. Am. Chem. Soc.* **1957**, *79*, 3937.
(14) Murakami, Y.; Maeda, M. *Biomacromolecules* **2005**, *6*, 2927.
(15) Ishizuka, N.; Hashimoto, Y.; Matsuo, Y.; Ijiro, K. *Colloids Surf., A* **2006**, *284−285*, 440.
(16) Topuz, F.; Okay, O. *Macromolecules* **2008**, *41*, 8847.
(17) Topuz, F.; Okay, O. *Biocromolecules* **2009**, *10*, 2652.
(18) We note that although the addition of TEMED into the DNA solution further increases the modulus of DNA gels (refs 16 and 17), no TEMED was used in the present study to prevent DNA denaturation.
(19) Flory, P. J. *Principles of Polymer Chemistry*; Cornell University Press: Ithaca, NY, 1953.
(20) Treloar, L. R. G. *The Physics of Rubber Elasticity*; Oxford University Press: Oxford, 1975.
(21) Stein, R. S.; Soni, V. K.; Yang, H.; Erman, B. In *Biological and Synthetic Networks*; Kramer, O., Ed.; Elsevier: Amsterdam, 1988; p 383.
(22) Shibayama, M. *Macromol. Chem. Phys.* **1998**, *199*, 1.
(23) Kizilay, M.; Okay, O. *Macromolecules* **2003**, *36*, 6856.
(24) Doi, M.; Edwards, S. F. *The Theory of Polymer Dynamics*; Clarendon Press: Oxford, 1989.
(25) Ogden, R. W.; Saccomandi, G.; Sgura, I. *Proc. R. Soc. London, Ser. A* **2006**, *462*, 749.
(26) Mark, J. E.; Erman, B. *Rubberlike Elasticity. A Molecular Primer*; Cambridge University Press: New York, 2007.
(27) We note that we did not employ any model here, such as the eight-chain model, etc.
(28) Smith, S. B.; Cui, Y..; Bustamante, C. *Science* **1996**, *271*, 795.
(29) Wang, M. D.; Yin, H.; Landick, R.; Gelles, J.; Block, S. M. *Biophys. J.* **1997**, *72*, 1335.
(30) Odijk, T. *Macromolecules* **1995**, *28*, 7016.
(31) Rouzina, I.; Bloomfield, V. A. *Biophys. J.* **2001**, *80*, 882.
(32) Blundell, J. R.; Terentjev, E. M. *Macromolecules* **2009**, *42*, 5388.
(33) Bauerle, S. A.; Hotta, A.; Gusev, A. A. *Polymer* **2005**, *46*, 4344.
(34) Hotta, A.; Clarke, S. M.; Terentjev, E. M. *Macromolecules* **2002**, *35*, 271.
(35) Serero, Y.; Jacobsen, V.; Berret, J.-F.; May, R. *Macromolecules* **2000**, *33*, 1841.
(36) Yziquel, F.; Carreau, P. J.; Tanguy, P. A. *Rheol. Acta* **1999**, *38*, 14.
(37) Rosenberg, B. H.; Cavalieri, L. F. *Biophys. J.* **1968**, *8*, 1138.
(38) Essevaz-Roulet, B.; Bockelmann, U.; Heslot, F. *Proc. Natl. Acad. Sci. U.S.A.* **1997**, *94*, 11935.
(39) Liphardt, J.; Onoa, B.; Smith, S. B.; Tinoco, I.; Bustamante, C. *Science* **2001**, *292*, 733.
(40) Bockelmann, U.; Thomen, P.; Essevaz-Roulet, B.; Viasnoff, V.; Heslot, F. *Biophy. J.* **2002**, *82*, 1537.
(41) Strick, T. R.; Allemand, J.-F.; Bensimon, D.; Croquette, V. *Annu. Rev. Biophys. Biomol. Struct.* **2000**, *29*, 523.